International Journal for Multiscale Computational Engineering, 16(2):131–142 (2018)

RANDOM WALK SIMULATION MODEL OF DIFFUSION IN CIRCULAR AND ELLIPTICAL PARTICULATE COMPOSITES

Jian Qiu & Yun-Bo Yi*

Department of Mechanical and Materials Engineering, University of Denver, Colorado 80208

*Address all correspondence to: Yun-Bo Yi, Department of Mechanical and Materials Engineering, University of Denver, Colorado 80208, E-mail: Yun-Bo.Yi @du.edu

Original Manuscript Submitted: 4/4/2017; Final Draft Received: 4/20/2018

We developed a random walk model for solving the diffusion problem arising from composite materials of particulate inclusions with different shapes. Our two-phase material system contains circular or elliptical impermeable inclusions that are randomly embedded in a matrix material. A computational algorithm was developed for random walk simulation of molecules and to estimate the effective diffusion coefficient of the composites. The random walk model has been validated by solutions from finite element analysis and effective medium theories. Our computational results show that the density of random distribution and the volume fraction of inclusions have significant effects on effective diffusion coefficients. Moreover, the aspect ratio of inclusions can significantly reduce diffusion speed when the volume fraction of inclusions is greater than $\sim$ *30%.*

KEY WORDS: *random walk, finite element analysis, heterogeneous materials, diffusion, Monte-Carlo method*

1. INTRODUCTION

Diffusion phenomena of heterogeneous materials have been widely studied, because the mechanical properties of composite materials can degrade in humid environments. Recently, carbon fiber–reinforced composites have been widely applied in the area of aerospace (Soutis, 2005), civil (Tavakkolizadeh and Saadatmanesh, 2003), and automotive (Rezaei et al., 2008) engineering, due to their light and strong properties. However, matrix materials such as resin or epoxy can absorb moisture from the surrounding environment, and water can diffuse in the matrix and degrade the matrix/reinforcement interface or interphase and reduce composite stiffness (Davies and Zhang, 1995). The diffusion coefficient is the most important parameter indicating diffusion behavior. Most of the techniques used to study the diffusion coefficient are analytical methods and finite element analysis (FEA). Maxwell–Garnett (MG) theory (Maxwell, 1873; Levy and Stroud, 1997) provides a method for predicting the effective diffusion coefficient for composite materials. In the MG model, a spherical inclusion is inserted into a circular shell of the matrix and assumes that the inclusion does not change the concentration field outside. Depending on the steady-state equation, the effective diffusion coefficient can be determined. However, the theory has some restrictions; for example, voids in the model cannot be impenetrable, and model equations are applicable for low-density systems only. Some researchers have provided solutions and improved MG theory (Gueribiz et al., 2009; Kalnin et al., 2002; Ruppin, 2000) to predict the effective diffusion coefficient for composite materials with impermeable inclusions. However, the shape of inclusions are merely spheres in three dimensions and circles in two dimensions. For some materials with large aspect ratios, no conclusion has been reached regarding the aspect ratio effect on the effective diffusion coefficient. Other approximations including the self-consistent approximation (Davis, 1977; Hill, 1965) and differential effective medium theory (Sheng, 1990) are widely used as well. However, most of these approximations have been found to be inaccurate if the system has a high-volume fraction of inclusions. Traditional numerical alternatives such as the finite element method (FEM) are widely used to overcome the difficulties involved in analytical approaches. Joliff

et al. (2013) developed a numerical model based on the FEM to analyze the diffusion coefficient of random carbon fibers distributed in a matrix. Tawerghi and Yi (2009) built a finite element model of a unit square plate containing both uniformly and randomly distributed circular voids to measure composite conductivity. Hou and Wu (1997) used the same method to study composite materials embedded with elliptical particles. Bakke and Øren (1997) presented a model describing ionic electrical conduction in porous media. However, modeling composite materials with finite element mesh requires thousands or even millions of nodes to solve the Laplace equation with sufficiently high accuracy, and this can be impractical when the particles have complex shapes (Qiu et al., 2015). Therefore, it is preferable to have a more efficient method to predict the effective diffusion coefficient. The random walk method is commonly used to estimate the diffusivity and conductivity of heterogeneous materials (Cukier et al., 1990; Tobochnik et al., 1990). This method is particularly useful because of its simple assumptions and mathematical formulation, Based on Brownian motion, it describes the stochastic diffusion of molecules traveling through space that is filled with other particles or physical barriers among continuous-time stochastic processes. One of its well-known applications is for estimating the diffusion coefficient in porous media made of an insulating matrix and pore space saturated with conducting fluid (Revil and Glover, 1997; Sahimi, 2011; Shankland and Waff, 1974). Other examples, including carbon fiber–reinforced epoxy-resin composites, can also be investigated by the random walk method (Wright, 1981). With inorganic reinforcing fiber, the amount of water that can be absorbed depends primarily on the chemical nature of the resin matrix and the environment to which it is exposed. This phenomenon can be best described as water molecules randomly moving in a resin matrix until they move out of the composite. Although the random walk method offers many benefits for the study of heterogeneous materials, most currently focus on simple geometries such as circular or square shapes, and inclusions in the system are usually arranged in an organized pattern (Tavakkolizadeh and Saadatmanesh, 2003; Trinh et al., 2000). It is our intention in the present study to extend the method to other applications involving more complex geometries, such as elliptical inclusions.

2. METHODS

2.1 Random Walk Method

2.1.1 Diffusion Coefficient of a Continuous Medium

The random walk model, the primary component of the entire study of the diffusion problem for heterogeneous materials, relies on the equivalence of Laplace's equation and the diffusion equation. In general, the diffusion of composite materials with impermeable inclusions can be described as a "walker" that randomly walks in the matrix phase of the composite with a constant diffusion coefficient. Particle diffusion in n-dimensional space can be described as Brownian motion, and the diffusion coefficient for isotropic materials in random walk theory can be calculated by mean-square displacement (MSD) of walker versus time. Using a sufficiently long amount of time, the diffusion coefficient of the matrix can be estimated by the following equation:

$$r^2 = 2nDt, \tag{1}$$

where r^2 is MSD, D is the diffusion coefficient of the system, t is the total random walk time, and n is the dimensional space in which the walker travels through the phase. MSD of a set of random walk step l_n, given by

$$r^2 = \frac{1}{N}\sum_{k=1}^{N} |l_k|^2, \tag{2}$$

where l is the length of each step, and N is the number of steps in the random walk simulation. In the two-dimensional (2D) case in which $n = 2$, we can convert Eq. (1) to

$$r^2 = 4Dt, \qquad t = N\tau, \tag{3}$$

where τ is the particle travel time for each step. Therefore,

$$D = \frac{1}{4N^2\tau}\sum_{k=1}^{N} |l_k|^2. \tag{4}$$

To make the same diffusion condition for comparing different methods and providing a dimensionless expression for the effective diffusion coefficient D_{eff}, we set a constant dimensionless step length $l = 0.001$ and a constant step time $\tau = 1$ s for the entire study. Depending on Eq. (4), we first measure the diffusion coefficient of matrix D_m as follows:

$$D_m = \frac{< r >^2}{4N}. \tag{5}$$

The relationship between MSD and diffusion time is linear, and the slope of the curve is the diffusion coefficient of the matrix. We allow a particle to randomly walk in a unit square and measure MSD at each time interval. Figure 1 shows MSD of random walks averaged from 1000 simulations, with relative error $< 1 \times 10^{-4}$. The number of steps Nranges from 0 to 2000. In Fig. 1, the blue line represents the value of r^2 and the red line the curve-fitting results. According to the curve-fitting results, we estimate the diffusion coefficient of the matrix to be 2.50334×10^{-5} s^{-1}.

In this study, we use the Monte-Carlo method to create a random system that contains all circular or elliptical inclusions randomly distributed in the matrix without overlapping one another. All of the inclusions are confined inside the unit square. To improve numerical efficiency for elliptically shaped voids, we create elliptical polygons with segments of equal length to represent the ellipses. Figure 2(a) shows two elliptical polygons, with the blue line representing polygons of ten segments and the red line representing a polygon of 100 segments. For accuracy, we used the 100-segment elliptical polygon in our model.

Our method differs from the simple lattice random walk (Vineyard, 1963), in that the molecules in our model move in an arbitrary orientation at each step, which represents a more realistic situation for diffusion. At each random walk step, a random number generator based on current time is used to generate a number between 0 and 1. Thus, a different set of random numbers is generated in each time step. The coordinates of the molecule at each step were computed from the following equations:

$$X_{i+1} = X_i + l \sin \alpha, \qquad Y_{i+1} = Y_i + l \cos \alpha, \tag{6}$$

where X and Y are the coordinates of molecules at each time step, and α is the angle of motion direction. Because all of the inclusions are impermeable, we developed an algorithm in which the molecules bounce back when they meet the inclusion–matrix interface. For the left and right sides of the plate, we assume that they are insulated. In other words, the molecules can only penetrate from bottom to top, and this is then reflected by the walls according to the law of reflection. Figure 2(b) shows that a single molecule moved one step and hit the surface of the elliptical

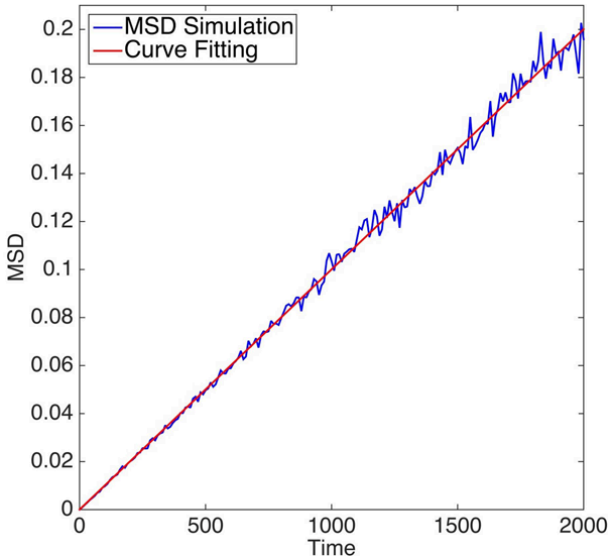

FIG. 1: MSD of random walks averaged from 1000 simulations in a 2D unit square

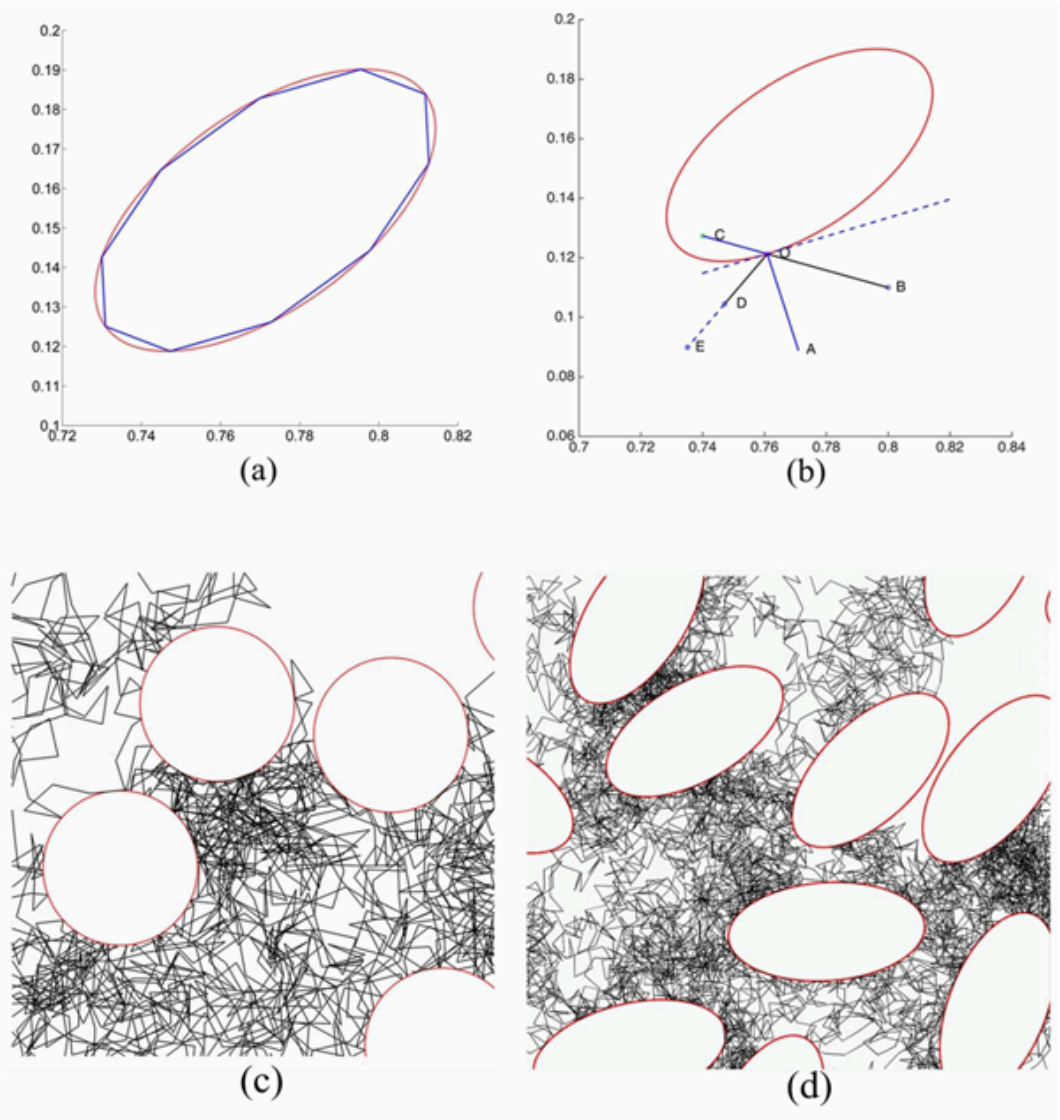

FIG. 2: (a) Elliptical polygon with ten and 100 line segments of equal length to represent the elliptical void; (b) trajectory of a molecule before and after it hits the elliptical polygon with 100 segments; (c) molecule bounced in the randomly distributed circular voids, with constant steps $l = 0.001$; (d) molecule bounced in the randomly distributed elliptical voids, with constant steps $l = 0.001$

inclusion. We determine the normal line (line OA) of the inclusion surface from the geometry of the elliptical polygon. In Fig. 2(b), we segment the ellipse with 100 straight lines, where OB is the incident path, OD the new path of the molecule, and OE the reflection path of OB. The algorithm checks the molecular position first. If the molecule meets the boundary of a polygon [e.g., OC in Fig. 2(b)], we implement the aforementioned algorithm to determine the angle of reflection according to the following equations:

$$\vec{n} = \frac{\overrightarrow{OA}}{\left\|\overrightarrow{OA}\right\|}, \tag{7}$$

$$\overrightarrow{OE} = \overrightarrow{OB} - 2(\overrightarrow{OB} \cdot \overrightarrow{n})\overrightarrow{n}, \tag{8}$$

$$\overrightarrow{OD} = \left\|\overrightarrow{OC}\right\| \frac{\overrightarrow{OE}}{\left\|\overrightarrow{OE}\right\|}. \tag{9}$$

Figure 2(c) shows the path of molecules when they reflect on the circular voids, and Fig. 2(d) shows the molecular path for ellipses when using the random walk algorithm.

At the beginning of a simulation, the molecule started from a random point on one side of the unit square and randomly walked in the system until it reached the opposite side or completed the prescribed maximum number of steps without reaching the opposite side of the square. We then recorded the total number of steps and repeated the simulation N times. In the end, we counted the number of trials that the molecule successfully reached the opposite side to represent the mass concentration. This process can be considered to be an approximation of a transient Fick's diffusion. Figure 3 shows an example of a successful random walk in a system with 40 circular inclusions, each with a radius of 0.05. The molecule started at the midpoint of one side of the square, and it took a total of 58,829 steps for the molecule to cross the entire system. The red line in the figure represents the trajectory of molecular movement.

2.2 Analytical Solution

To verify the random walk model, we used some existing approximate solutions found in the literature. For example, the MG equation can be used to estimate the effective diffusion coefficient in a two-phase composite as follows:

$$D_{eff} = D_m \left[1 + \frac{d(D_f - D_m)V_f}{D_f + (d-1)D_m - (D_f - D_m)V_f}\right]. \tag{10}$$

In this equation, D_m and D_f are the diffusion coefficients of the two phases, V_f is the volume fraction of the inclusions, and d represents the system dimension; in the 2D system, d is equal to 2. However, it is well known that the standard MG method is inaccurate when inclusions are impenetrable. For impermeable inclusions, an improved

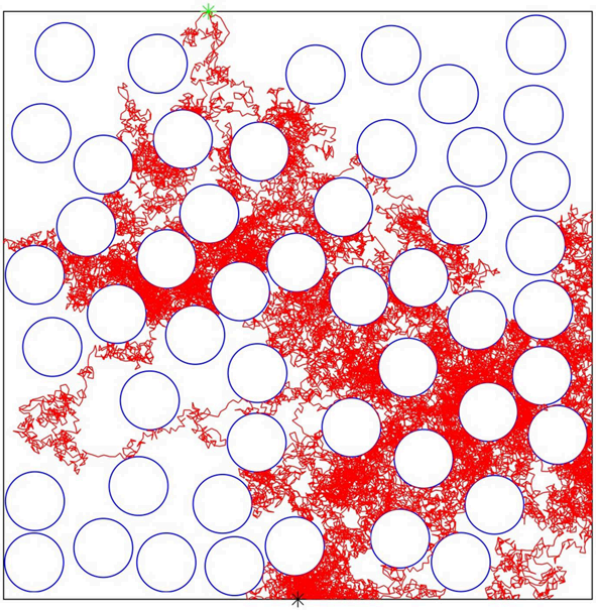

FIG. 3: Set of vertices visited by a 2D random walk in circular voids with a volume fraction of 31.41%. The walker began at the center of the box, and after 58,829 steps, it reached the boundary.

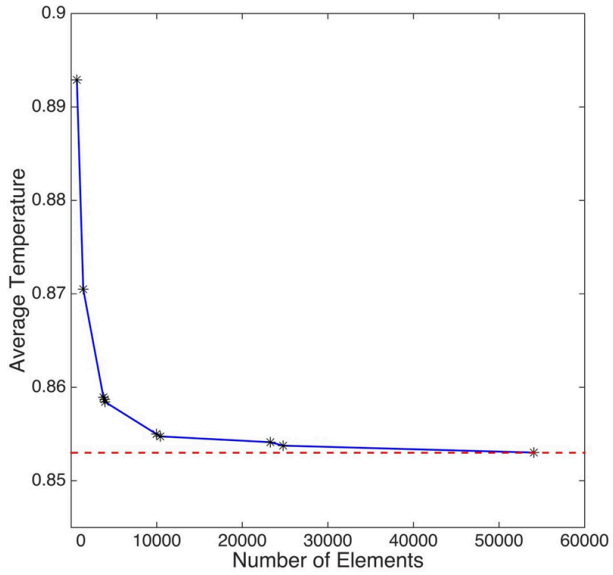

FIG. 4: Convergence of finite element model–average temperature as a function of element number

method was developed by Kalnin et al. (2002). With this method, instead of considering the concentration of diffusing particles in the matrix as equal to the effective medium, these authors introduced a parameter λ, where, for impenetrable inclusions,

$$\lambda = \frac{1}{1 - V_f}. \tag{11}$$

With this modification, the improved MG method for impenetrable inclusions can be summarized in Eqs. (12) and (13) in two dimensions as follows:

$$D_{eff} = D_m \lambda \left[1 + \frac{d(D_m\lambda - D_f)V_f}{\lambda D_f + (d-1)D_m - (\lambda D_f - D_m)V_f} \right], \tag{12}$$

$$D_{eff} = \frac{D_m}{1 - V_f} \left[1 - \frac{2V_f}{1 + V_f} \right], \tag{13}$$

where V_f is the volume fraction of the inclusions, and D_m is the diffusion coefficient of the matrix. To compare the analytical method with numerical methods, we treated D_m as a constant ($D_m = 2.50334 \times 10^{-5}$ s^{-1}), which we explain in the previous discussion.

Bruggman's effective medium (BEM) model (Bruggeman, 1935) also provides an acceptable approximation of macroscopic properties of composite materials at lower-volume fractions of inclusions. For a two-phase system, the equation may be shown as

$$V_f \frac{D_f - D_{eff}}{D_f + (d-1)D_{eff}} + (1 - V_f) \frac{D_m - D_{eff}}{D_m + (d-1)D_{eff}} = 0, \tag{14}$$

$$D_{eff} = (1 - 2V_f)D_m. \tag{15}$$

2.3 FEM

2.3.1 Element Generation and Partition

In this study, we use FEA to validate the random walk model. To generate a system of randomly distributed nonoverlapping circles or ellipses in a unit square, we develop a dynamic collision algorithm on the basis of C-programming

language (Bell Labs, Murray Hill, New Jersey) to fully disperse the inclusions. We generate three-node triangular shell elements for thermal analysis in the matrix using MatrixLaboratory (MATLAB; MathWorks, Natick, Massachusetts) and COMSOL Multiphysics (COMSOL Inc., Stockholm, Sweden). The mesh density of the model depends on the curvature of the geometry. Therefore, in MATLAB a few parameters including the curvature cutoff threshold and maximum element size are defined to avoid excessive local elements and numerical inaccuracy induced by local singularities. Figure 4 shows the convergence of results based on a model containing 30 circular inclusions, each with a radius of 0.5. The x-axis is the total number of elements in the model, and the y-axis represents the average nodal temperature at the top of the model. In the simulation, we choose a mesh quality of ~ 0.4 with ~ 6000 to 8000 elements for the model of circular inclusions and 13,000 to 20,000 elements for the model of elliptical inclusions. Each simulation deviates from the convergent result with an error of $< 0.5\%$. Mesh data such as nodal positions and element compositions are contained in an ABAQUS© (Dassault Systèmes Simulia Corp., Rhode Island) script file. To maintain consistency with parameters used in the random walk model, we set the matrix diffusion coefficient in the FEA (K_m) to 2.5344×10^{-5} s^{-1} and the thermal coefficient of inclusions K_f to 0. For convenience, the density and specific heat of the matrix are set to 1. A unit temperature was defined on the bottom of the domain, and the remaining three sides are insulated. No kinetic degrees of freedom are present in the elements, and the temperature is the only remaining degree of freedom. Thermal conduction occurs due to the temperature gradient, and the steady-state solution was sought from the Laplace equation. We compute the average temperature at the top of the unit square. Because diffusion transfer and heat transfer have the same governing equation, we use average node temperature to represent concentration of mass in the model.

2.3.2 Finite Element Model

We use ABAQUS to analyze the transient heat transfer process in the model. We study circular and elliptical inclusions, and all inclusions are the same size. Figure 5(a) shows the finite element mesh for the model of 30 circular inclusions, each with a radius of 0.5. The number of triangular elements in the model is 6353. Figure 5(b) shows an example of randomly distributed elliptical inclusions with 14,132 elements. Semimajor axis length is 0.6 and semiminor axis length 0.3.

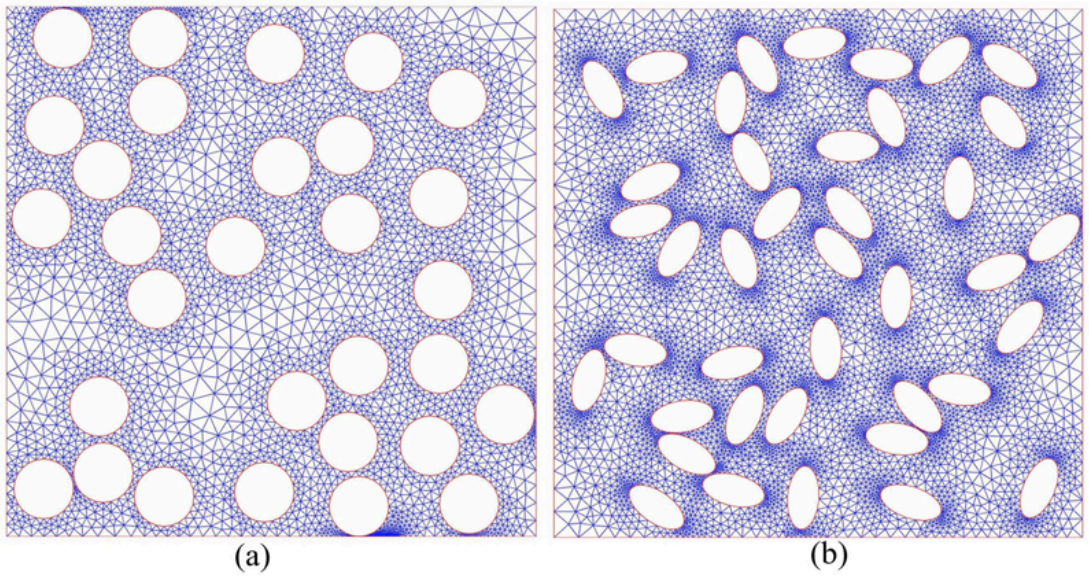

FIG. 5: Finite element model of (a) circular voids randomly distributed in the plate with a 23.56% volume fraction and (b) elliptical voids randomly distributed in the plate with a 17.67% volume fraction

3. RESULTS AND DISCUSSION

3.1 MSD

To measure MSD of circular and elliptical void models, we started with ordinary diffusion inside a simulation box of unit width surrounded by rigid walls. According to Eq. (5), the diffusion coefficient of the system is a linear function of diffusion time with constant step size. Because fixed step length l and step time τ can determine the diffusion coefficient of the matrix D_m, as discussed in Eqs. (2)–(5), the only variable that can affect the effective diffusion coefficient is the volume fraction of impermeable inclusions in the entire system. We varied the volume fraction of inclusions from 0.1 to 0.5, with a fixed step size $l = 0.001$ and step time $\tau = 1$ s. We ran the simulation 1000 times every 50 s and measured MSD at each time interval. We examined both types of inclusions (ellipses and circles). Collected data were analyzed based on the curve-fitting technique. Figure 6 shows MSD for the elliptical model as a function of observation time t for three different volume fractions ($V_f = 0.1$, 0.3, and 0.5). The aspect ratio (major axis length to minor axis length) of elliptical voids was 2. Diffusion time ranged from 0 to 50,000 s. The variance of MSD initially follows the behavior of normal diffusion, such that MSD increases in proportion to t, following Eq. (5). After a long period of time, MSDs approach a constant value. MSD saturates, and because of the confinement in the box, we only measured the linear parts of the curves and found the effective diffusion coefficient of the systems. In Fig. 6, the red lines show curve-fitting results using linear least-squares regression.

3.2 Comparisons between FEA and Random Walk

To verify the random walk simulations, we used two different volume fractions of voids in the system, with the radius of inclusions $r = 0.02$. The higher-volume fraction of voids is 0.5, and the lower fraction is 0.2. We fixed step size at $l = 0.001$ and ran the simulation 1000 times at each time interval. Diffusion time ranged from 0 to 5000, with a constant time interval $t_0 = 100$ s. We measured the number of molecules that moved out of the system and calculated the mass concentration at the top of the square. According to mass transfer theory, the molecules that moved out of the system were equivalent to the mass concentration. We then used the same parameters to create a random system and measured the temperature in the finite element model. Because heat transfer and mass transfer have the same

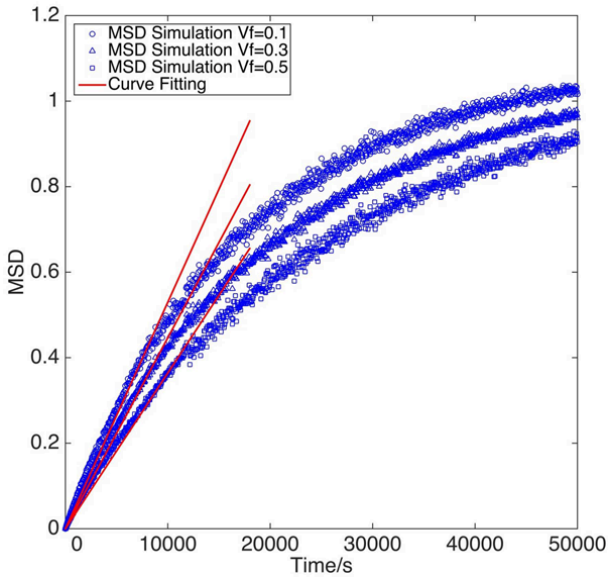

FIG. 6: MSD of random walks averaged from 1000 simulations, with different volume fractions of elliptical voids ranging from 0.1 to 0.5. Slopes of regression lines are 2.2817×10^{-5} s^{-1} for $v_f = 0.1$, 1.8722×10^{-5} s^{-1} for $v_f = 0.3$, and 1.4847×10^{-5} s^{-1} for $v_f = 0.5$.

governing equation, the results are analogous under the same conditions. We ran 20 simulations at each time interval. Figure 7(a) shows results for both random walk and finite element models. Squares and circles represent average temperature and concentration of mass at the end of the simulation, respectively. Red and blue lines represent curve-fitting results. We obtained very close results from both methods: The difference between the two results was < 2. The findings imply that under the same conditions, both methods apply to systems using a wide range of volume fractions.

3.3 Elliptical Voids

To investigate the effective diffusion coefficient of the elliptical inclusions composite, we fixed parameters at $a = 0.1$ and $b = 0.05$, with total volume fraction of the inclusions at 0.2 and 0.5. Random walk step size $l = 0.001$, and time step $\tau = 1$ s. Diffusion time ranged from 0 to 5000 s, with a constant time interval $t_0 = 100$ s. At each time interval, we ran the simulation 1000 times and measured the concentration of mass at the top surface of the model. For FEA, we ran the simulation 20 times at each time interval, using the same conditions as those in the random walk. Figure 7(b) shows FEA and random walk results from the system of elliptical inclusions. Circles and squares represent simulation results from FEA and random walk, respectively. The red and and blue lines show curve-fitting results. Mass concentration increased with time and reached a constant value after a sufficiently long simulation. The difference between these two methods was 0.2%. According to Figs. 7(a) and 7(b), we found our algorithm to be effective for both elliptical and circular inclusions and confirmed that heat and mass transfers behave similarly in composite materials.

A more indicative view of these two phenomena can be observed in Fig. 8, which shows a comparison between ABAQUS analysis and random walk simulation. In Figs. 8(a) and 8(b), we used the same number, sizes, and orientations of elliptical inclusions and found good agreement between the two methods. Figure 8(a) shows temperature distribution from FEA. Because the model contains impermeable random inclusions, the temperature gradient was not uniformly distributed. We also found that the temperatures were greater in those locations with higher concentrations of inclusions. This is because impermeable inclusions block the pathway of heat flow in the congregating area, leading to localized high temperatures. Figure 8(b) shows the distribution of equivalent mass concentration based on the random walk model. The darker red area in Fig. 8(b) represents a higher mass concentration, whereas the darker blue area shows a smaller mass concentration.

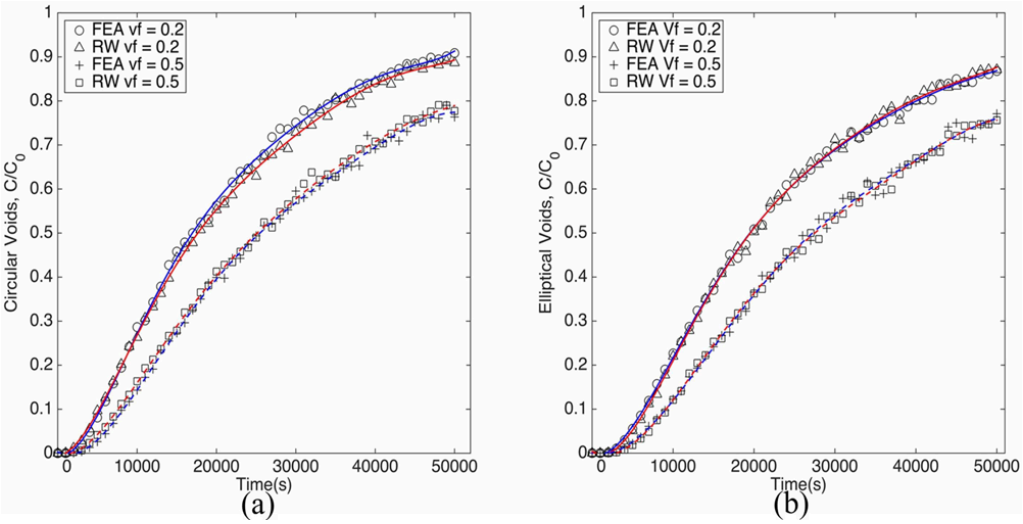

FIG. 7: Comparison of concentration ratio between FEA and random walk method for (a) circular voids with volume fractions between 0.2 and 0.5; (b) elliptical voids with volume fractions between 0.2 and 0.5

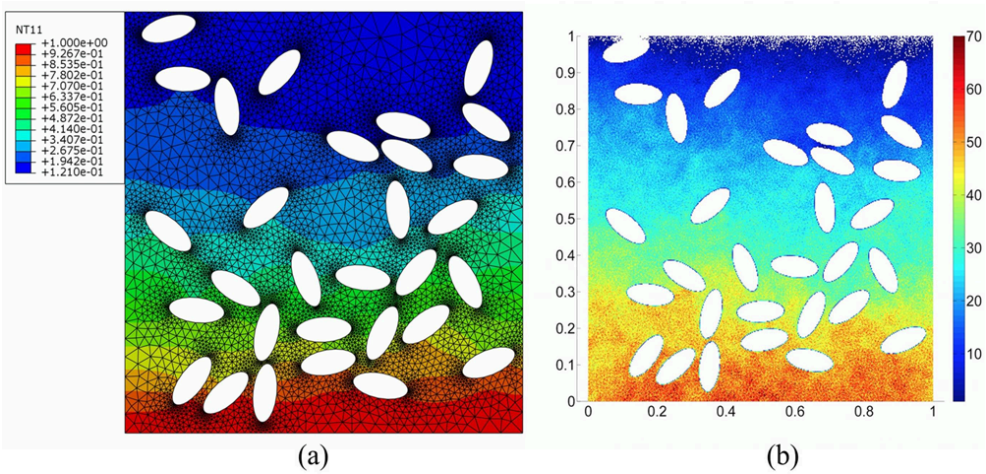

FIG. 8: (a) Temperature distribution obtained from FEA; (b) simulated mass concentration using the random walk model

3.4 Aspect Ratio Effect

It is well known that inclusions of large aspect ratios can significantly affect the diffusion coefficient. We investigated the effective diffusion coefficient by comparing elliptical and circular inclusions at the same volume fractions using the random walk model. In the circular inclusion system, we fixed the radius at $r = 0.1$, and in the elliptical inclusions system, we varied the aspect ratio a/b from 0.1 to 0.5, where a is the semimajor axis and b the semiminor axis. We varied the volume fraction from 0.1 to 0.5 and measured the concentration of mass at different time intervals. Figure 9(a) shows a comparison of concentration ratios between elliptical and circular inclusions at different volume fractions. Solid and dotted lines represent curve-fitting results for circular and elliptical inclusions, respectively. At a lower-volume fraction, the aspect ratio of inclusions has an insignificant effect on the diffusion coefficient. However, when the volume fraction increases to a higher value, such as 0.3 or 0.5, elliptical inclusions have a smaller concentration, that is, a lower effective diffusion coefficient as compared to the circular system. This is because at a lower volume fraction, the system has enough space for the molecules to move and diffuse. When the number of inclusions

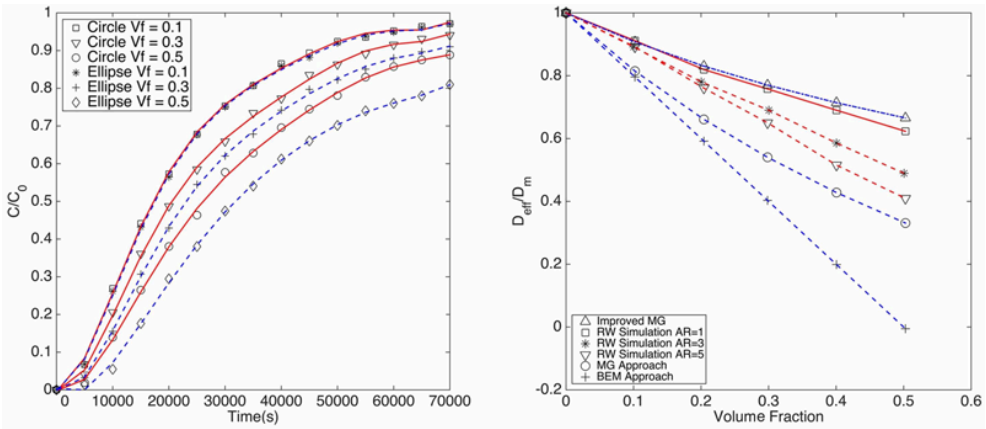

FIG. 9: (a) Effect of aspect ratio on the concentration ratio for different volume fractions; (b) comparison of dimensionless effective diffusion coefficient between analytical solutions and computer simulations for randomly distributed voids with different aspect ratios. (Solid line) Circular voids; (dashed line) elliptical voids with aspect ratios of 3 and 5.

increases, molecules hit the inclusions more frequently. The molecules tend to be "trapped" in the vicinity of higher aspect ratio inclusions, and it takes longer for a molecule to "escape" the region. Figure 9(b) shows a comparison between the generally accepted MG solution and computer simulations for randomly distributed inclusions in terms of the dimensionless diffusion coefficient. Squares and stars are simulation results with different aspect ratios, and triangles and circles are analytical results with different volume fractions of inclusions. The immediate conclusion that may be drawn from Fig. 9(b) is that the effective diffusion coefficient decreases with the volume fraction of inclusions. A lower-volume fraction of inclusions slightly affects the effective diffusion coefficient of the system, where $v_f = 0.1$ and 0.2. However, at a volume fraction as high as $v_f = 0.3$ or 0.5, the effective diffusion coefficient significantly decreases. Compared to simulation results, the decreasing rate of the effective diffusion coefficient does not change, because the analytical solution does not consider that the molecule can collide more frequently in a localized region with inclusions of higher aspect ratio. It should be pointed out here that the MG equation and BEM approximation yield rather inaccurate results, especially at higher-volume fractions, because they (1) neglect the different concentrations in the inclusions and the matrix and (2) cannot precisely predict the effective diffusion coefficient at a high-volume fraction.

4. CONCLUSIONS

In this research, we developed an efficient random walk algorithm that describes the motion of molecules in a 2D heterogeneous medium with both circular and elliptical inclusions. The main advantage of this algorithm is its simplicity and computational efficiency in comparison to the FEM. In addition, it accurately simulates the Brownian motion of molecules in a random particulate system, even when the system has a high-volume fraction of inclusions. Our random walk simulation results agree very well with the FEM for both circular and elliptical systems. At a lower-volume fraction, for example, at 10%, random walk results also agree with analytical solutions. However, when the volume fraction is sufficiently high, for example, greater than 30%, there is an apparent discrepancy between simulation results and the analytical solution, mainly because all of the effective medium approximations can only deal with lower-volume fraction systems. At higher-volume fractions, the geometric shape of inclusions has an important role in the effective diffusion coefficient. A higher aspect ratio of impenetrable inclusions can reduce the speed of diffusion, because it increases the probability of collision between the molecules and solid interfaces.

REFERENCES

Bakke, S. and Øren, P.E., 3-D Pore-Scale Modelling of Sandstones and Flow Simulations in the Pore Networks, *SPE J.*, vol. **2**, pp. 136–149, 1997.

Bruggeman, V.D., Berechnung Verschiedener Physikalischer Konstanten von Heterogenen Substanzen. I. Dielektrizitätskonstanten und LeitfÄHigkeiten Der Mischkörper aus Isotropen Substanzen, *Annalen Physik*, vol. **4**, pp. 636–664, 1935.

Cukier, R.I., Sheu, S.Y., and Tobochnik, J., Random-Walk Simulation of the Dielectric Constant of a Composite Material, *Phys. Rev. B*, vol. **42**, pp. 5342–5344, 1990.

Davies, G.A.O. and Zhang, X., Impact Damage Prediction in Carbon Composite Structures, *Int. J. Impact Eng.*, vol. **16**, pp. 149–170, 1995.

Davis, H., The Effective Medium Theory of Diffusion in Composite Media, *J. Amer. Ceram. Soc.*, vol. **60**, pp. 499–501, 1977.

Gueribiz, D., Rahmani, M., Jacquemin, F., Fréour, S., Guillen, R., and Loucif, K., Homogenization of Moisture Diffusing Behavior of Composite Materials with Impermeable or Permeable Fibers—Application to Porous Composite Materials, *J. Comp. Mater.*, vol. **43**, pp. 1391–1408, 2009.

Hill, R., A Self-Consistent Mechanics of Composite Materials, *J. Mech. Phys. Solids*, vol. **13**, pp. 213–222, 1965.

Hou, T.Y. and Wu, X.H., A Multiscale Finite Element Method for Elliptic Problems in Composite Materials and Porous Media, *J. Comput. Phys.*, vol. **134**, pp. 169–189, 1997.

Joliff, Y., Belec, L., and Chailan, J.F., Modified Water Diffusion Kinetics in a Unidirectional Glass/Fibre Composite due to the Interphase Area: Experimental, Analytical and Numerical Approach, *Comp. Struct.*, vol. **97**, pp. 296–303, 2013.

Kalnin, J.R., Kotomin, E.A., and Maier, J., Calculations of the Effective Diffusion Coefficient for Inhomogeneous Media, *J. Phys. Chem. Solids*, vol. **63**, pp. 449–456, 2002.

Levy, O. and Stroud, D., Maxwell Garnett Theory for Mixtures of Anisotropic Inclusions: Application to Conducting Polymers, *Phys. Rev. B*, vol. **56**, pp. 8035–8046, 1997.

Maxwell, J.C., *A Treatise on Electricity and Magnetism*, Oxford, UK: Clarendon Press, 1873.

Qiu, J., Yi, Y.B., and Guo, X., Computational Prediction of Electrical and Thermal Conductivities of Disklike Particulate Composites, *Int. J. Comput. Mater. Sci. Eng.*, vol. **4**, p. 1550013, 2015.

Revil, A. and Glover, P.W.J., Theory of Ionic-Surface Electrical Conduction in Porous Media, *Phys. Rev. B*, vol. **55**, pp. 1757–1773, 1997.

Rezaei, F., Yunus, R., Ibrahim, N.A., and Mahdi, E.S., Development of Short Carbon Fiber-Reinforced Polypropylene Composite for Car Bonnet, *Poly. Plast. Technol. Eng.*, vol. **47**, pp. 351–357, 2008.

Ruppin, R., Evaluation of Extended Maxwell-Garnett Theories, *Opt. Comm.*, vol. **182**, pp. 273–279, 2000.

Sahimi, M., *Flow and Transport in Porous Media and Fractured Rock: From Classical Methods to Modern Approaches*, New York, NY: John Wiley & Sons, 2011.

Shankland, T.J. and Waff, H.S., Conductivity in Fluid-Bearing Rocks, *J. Geophys. Res.*, vol. **79**, pp. 4863–4868, 1974.

Sheng, P., Effective-Medium Theory of Sedimentary Rocks, *Phys. Rev. B*, vol. **41**, pp. 4507–4512, 1990.

Soutis, C., Carbon Fiber Reinforced Plastics in Aircraft Construction, *Mater. Sci. Eng. A*, vol. **412**, pp. 171–176, 2005.

Tavakkolizadeh, M. and Saadatmanesh, H., Strengthening of Steel-Concrete Composite Girders using Carbon Fiber Reinforced Polymers Sheets, *J. Struct. Eng.*, vol. **129**, pp. 30–40, 2003.

Tawerghi, E. and Yi, Y.B., A Computational Study on the Effective Properties of Heterogeneous Random Media Containing Particulate Inclusions, *J. Phys. D Appl. Phys.*, vol. **42**, no. 175409, pp. 1–10, 2009.

Tobochnik, J., Laing, D., and Wilson, G., Random-Walk Calculation of Conductivity in Continuum Percolation, *Phys. Rev. A*, vol. **4**, pp. 3052–3058, 1990.

Trinh, S., Arce, P., and Locke, B.R., Effective Diffusivities of Point-Like Molecules in Isotropic Porous Media by Monte Carlo Simulation, *Trans. Porous Media*, vol. **38**, pp. 241–259, 2000.

Vineyard, G.H., The Number of Distinct Sites Visited in a Random Walk on a Lattice, *J. Mathemat. Phys.*, vol. **4**, pp. 1191–1193, 1963.

Wright, W.W., The Effect of Diffusion of Water into Epoxy Resins and Their Carbon-Fibre Reinforced Composites, *Composites*, vol. **12**, no. 3, pp. 201–205, 1981.